

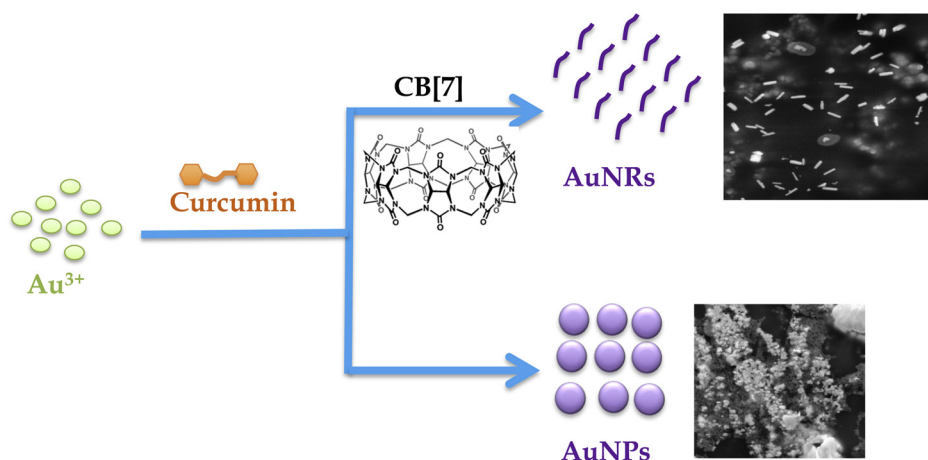
Capping of supramolecular curcubit[7]uril facilitates formation of Au nanorods during pre-reduction by curcumin

Riham El Kurdi, Digambara Patra*

Department of Chemistry, American University of Beirut, Beirut, Lebanon



GRAPHICAL ABSTRACT



ARTICLE INFO

Keywords:

Au
Nanoparticles
Nanorods
Curcumin
Curcubit[7]uril

ABSTRACT

Curcumin being biologically available and non-toxic natural compound is an attractive and alternative green reagent for the reduction of gold salts to elemental gold. Here, we bring new insight that shape and size of the Au nanoparticles (NPs) can be tuned by using curcumin in combination with supramolecular host molecule such as curcubit[7]uril (CB[7]) as stabilizing agent. It is found that AuNPs prepared using curcumin alone in aqueous environment gives spherical and smaller size, 10–20 nm, particles with its surface Plasmon resonance peak at ~536 nm. At the same time when CB[7] is used as a capping agent along with curcumin, larger size NPs and at higher concentration (~50 μM) of CB[7] Au nanorods (NRs) are formed with a broad surface Plasmon resonance spectrum peaked at ~610 nm. Thus, CB[7] at higher concentration ultimately helps to form Au NRs. Formation of AuNPs and AuNRs has been confirmed by XRD and conjugation of CB[7] and curcumin is established by FT-IR and TGA data. However, these particles aggregate in solution to form particles between 200 nm and 300 nm with a polydispersity of 0.25 as observed in DLS. Zeta potential measurement indicates formation of stable nanoparticles/nanorods without further precipitation within time. Kinetic study shows that the half-life for the formation of AuNP/NRs is ~36 min, whereas degradation of curcumin during synthesis has a half-life of ~10 min, this discrepancy suggests some amount of curcumin degrades on its own during this process besides acting as reducing agent.

* Corresponding author.

E-mail address: dp03@aub.edu.lb (D. Patra).

<https://doi.org/10.1016/j.colsurfa.2018.05.022>

Received 27 February 2018; Received in revised form 8 May 2018; Accepted 8 May 2018

Available online 09 May 2018

0927-7757/ © 2018 Elsevier B.V. All rights reserved.

1. Introduction

Gold nanoparticles are categorized depending on the shapes. Nanospheres, nanorods, nanowires, nanoshells, nanocages etc. have been widely employed in bio-nanotechnology based on their unique properties and multiple surface functionalities [1–4]. To control the shape and size, synthesis techniques are continuously getting developed for many years. Au nanospheres/nanowires can be easily synthesized by reducing aqueous tetrachloroauric (III) acid trihydrate (HAuCl_4) solution using reducing agents under different parameters and conditions [5,6]. Au nanorods synthesis can also be performed using electrochemical deposition of Au within the pores of nanoporous polycarbonate or alumina membranes [7]. Au nanoshells are referred as a type of spherical nanoparticle with a dielectric core which is covered by a thin metallic shell [8] whereas Au nanocages are based on the galvanic replacement reaction of truncated silver nanocubes and aqueous HAuCl_4 [9]. Gold nanoparticles are characterized by their small diameter with large surface-to-volume ratio, unique physical and chemical properties that can be changed according to requirements of size, composition and shape. In addition AuNPs present high robustness and quantitative and qualitative target binding properties [10].

In contrast to the host–guest chemistry of α -, β -, and γ cyclodextrin which has developed steadily over the past century, the supramolecular chemistry of cucurbit[6]uril, (CB[6]) only began to develop in the 1980s and 1990s [11]. Interest in the CB[n] family has increased dramatically leading to the preparation of four new CB[n] homologues (CB [5], CB[7], CB[8], and CB[10]) by the research groups of Kim and Day [12,13]. CBs are very useful building blocks in the preparation of nanomaterials. Therefore, numerous studies on the host–guest chemistry of CB homologues and their recognition properties were published [11,14,15]. CBs present two identical portals decorated with partially negatively charged carbonyl groups and rigid symmetrical structures, leaving them as a unique capping agents to stabilize the gold nanoparticles in the aqueous solutions [16]. Corma et al. were the first to provide the synthesis of CB-containing gold nanoparticles [17]. Premkumar et al. reported the formation of water dispersible gold nanoparticles in the presence of CB[7] without using any capping agent [18]. Lee et al. have prepared CB [5] capped gold nanoparticles by reducing HAuCl_4 with NaBH_4 in the presence of various amounts of CB [5] [19]. Biosynthesis of gold nanoparticles with extract of plants including curcumin [6,20,21], lemongrass [22], aloe vera [23] and tamarind leaf [24] has been developed frequently. Curcumin, a polyphenol derived from turmeric plant, is widely used in medicinal application and food preparation in south-east Asia, China and India [25]. In order to increase the bioavailability of curcumin, different methods have been used for conjugation of curcumin to nanoparticles, particularly, in aqueous media that improve its activity, half-life and stability [25]. In this paper we have developed a new one pot green synthesis method of gold nanoparticles facilitated by curcumin as reducing agent and cucurbit [7] uril as a capping and stabilizing agent. The procedure is green because it uses non-toxic spice, curcumin, and avoids toxic chemicals and harmful solvents during reduction reaction for the preparation of gold nanoparticles. Kinetics and thermodynamics during synthesis of curcumin mediated cucurbit[7]uril capped gold nanoparticles have been investigated.

2. Materials and methods

2.1. Materials

Tetrachloroauric (III) acid trihydrate (HAuCl_4) was obtained from Acros. Curcumin and cucurbit[7]uril were purchased from Sigma Aldrich. All the chemicals were used without further purification and dissolved in double distilled water except that stock of curcumin (received from Sigma Aldrich) was prepared in methanol.

2.2. Synthesis of stabilized cucurbit[7]uril gold nanoparticles/rods

The synthesis was carried out in basic aqueous media since cucurbit [7]uril is insoluble in double distilled water. First of all, 50 μM of CB[7] were dissolved in 1 mL NaOH solution then 14 mL of double distilled water were added and left for 15 min at 45 °C. Second of all, 1 mM of HAuCl_4 dissolved in 15 mL of double distilled water was added. Curcumin at 10 mM was mixed to the solution at the end. To finalize and to precipitate the gold, the final solution was centrifuged at 15,000 rpm for 25 min at 35 °C.

2.3. Characterization and spectroscopic analysis

Scanning electron microscopy (SEM) analysis was done using Tescan, Vega 3 LMU with Oxford EDX detector (Inca XmaW20). Briefly, few drops of gold solution were settled on an aluminum stub and coated with carbon conductive adhesive tape. Zeta potential value and particle size distribution were measured using Particulate systems, NanoPlus Zeta Potential/Nano Particle analyzer. The absorption spectra were recorded at room temperature using a JASCO V-570 UV–VIS–NIR spectrophotometer. The synchronous fluorescence measurements were documented with resolution increment 1 nm and slit 5 nm using Jobin-Yvon-Horiba Fluorolog III fluorometer and the FluorEssence program. The excitation source was a 100 W Xenon lamp, and the detector used was R-928 operating at a voltage of 950 V. To record resonance Rayleigh scattering spectrum, synchronous fluorescence scan was measured using the same instrument by keeping the excitation and emission wavelength interval at 0 nm. Synchronous fluorescence scan measurement was carried out in suspension of gold nanoparticles using a 10 mm cuvette at 90° sample geometry.

Thermogravimetric Analysis (TGA) was done using a Netzsch TGA 209 in the temperature range 30–800 °C with an increment of 10 °C/min in a N_2 atmosphere. The X-Ray diffraction (XRD) data were collected using a Bruker d8 discover X-Ray diffractometer equipped with Cu-K α radiation ($\lambda = 1.5405 \text{ \AA}$). The monochromator used was Johansson Type. The step size was 0.02 s and the scan rate was 20 s per step.

3. Results and discussion

Gold nanoparticles/nanorods were prepared through one pot green synthesis mixing HAuCl_4 with cucurbit[7]uril and curcumin in aqueous media. To demonstrate the role of CB[7] and curcumin as surfactant/stabilizing and reducing agent respectively, two different experiments were carried out with/without curcumin. The difference between the two experiments was obvious as is noticed in Fig. 1A & B. In fact, after 24 h, in both cases, with and without curcumin, AuNPs/AuNRs were formed and this was observed from the color change of the solution. Hence, the difference was remarkable as in the absence of curcumin the color was slightly changed, whereas in the presence of curcumin the color turned from orange to dark grey (Fig. 1A). The color change was later on confirmed by centrifuging, where in absence of curcumin small amount of AuNPs was precipitated (Fig. 1B). Hence, it can be deduced that the carbonyl groups in CB[7] contribute to the formation of stable host-guest inclusion complexes with HAuCl_4 ; therefore, CB[7] presents high affinity inducing stable AuNPs reduced by curcumin. This stabilizing effect was verified by Gürbüz et al. where they had indicated that CBs act as a capping agent to stabilize the gold nanoparticles in the aqueous solutions [16]. The resulted AuNPs were monitored by Resonance Rayleigh Scattering (RRS) and UV–vis absorption spectra. The RRS spectrum was measured by applying synchronous fluorescence spectroscopy (SFS) by keeping the wavelength interval ($\Delta\lambda$) at 0 nm. The resulted spectrum is depicted in Fig. 2A. For the formed AuNPs, three peaks were obtained; two major SPR peak at ~435 nm and at ~550 nm and a minor peak at ~380 nm. The UV–vis absorption spectrum for gold nanoparticles is shown in Fig. 2B. The absorption

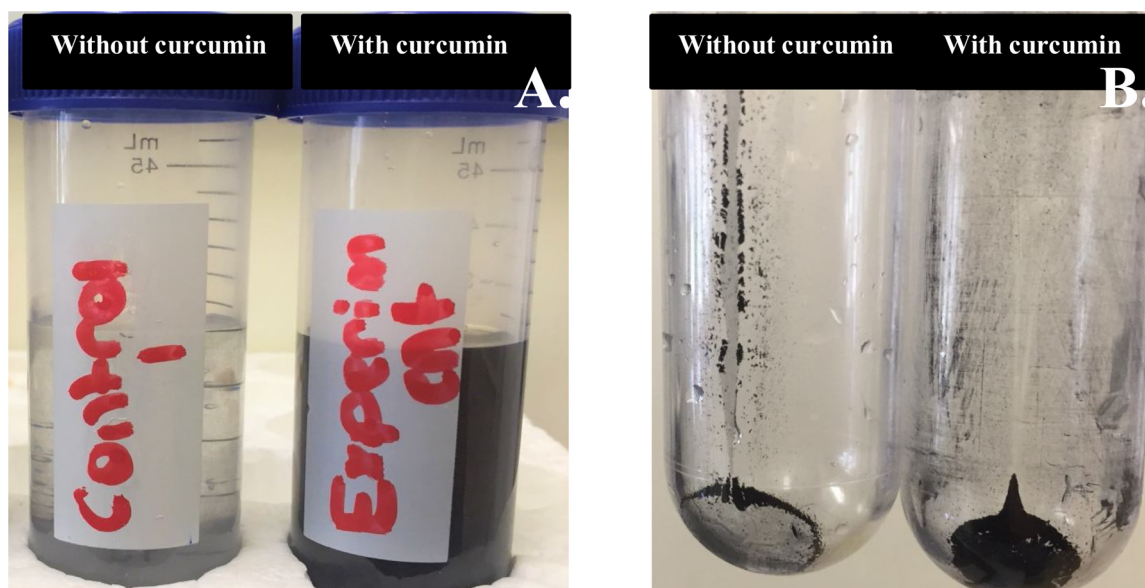


Fig. 1. Color change of the solution after 24 h (A) and quantity of precipitated gold nanoparticles after centrifuging (B) with/without curcumin.

spectrum for AuNPs is characterized by a broad band in the visible region with a surface SPR peak at ~ 610 nm. Abdulwahab et al. [26] had demonstrated that the sharp peaks indicate the formation of spherical nanoparticles. To identify the shape of the formed gold nanoparticles, SEM technique was applied. The images were shown in Fig. 3A & B. It can be seen from the images that Au nanoparticles are little bit spherical in shape (10–20 nm) with smooth surface in addition to the formation of Au nanorods which explain the broadness of the peak. The formation of AuNPs/AuNRs was verified by EDX analysis, where EDX spectrum demonstrated the presence of Au peaks and carbon peak as expected due to capping of cucurbituril/curcumin (see Fig. 3).

By varying the cavity size of the CBs and their ability to accommodate more than one guest in their cavity, the rigid symmetrical structure allowed the preparation of different shape of nanometals such as nanoparticles, nanocomposites, vesicles and rods [16]. This hypothesis was confirmed while studying the effect of CB[6] on the particle size. It was observed that CB[6] produced larger particles (shown in Fig. 3D) compared to presence of CB[7]. Subsequently, effect of concentration of CB[7] was investigated for which five different concentrations of 0, 5, 10, 25 and 50 μM were studied and the results are described below.

The RRS spectra of CB[7] stabilized AuNPs/AuNRs prepared at different concentration of CB[7] is depicted in Fig. 4A. For all the concentrations, the formed AuNPs/AuNRs gave two major SPR peaks,

at ~ 435 nm and at ~ 550 nm with a minor peak at ~ 380 nm. However, increasing the concentration of CB[7] during synthesis enhanced the intensity of the SPR peak. Hence, for 50 μM the highest intensity was obtained. Remarkable difference was obtained when UV–vis spectra were measured. As is seen in Fig. 4B, in the absence of CB[7], a clear and sharp peak was obtained at ~ 536 nm. However, in the presence of low concentration (5 and 10 μM) of CB[7], the absorbance at ~ 536 nm started decreasing and a new peak started appearing at ~ 610 nm. Further increase in CB[7] concentration (to 25 and 50 μM) during synthesis of AuNPs, gave a broad spectrum peaked at ~ 610 nm. This shift is the cause of the formation of different shape and size of AuNPs/AuNRs. Hence, this was verified by SEM images depicted in Fig. 5A–E. It is clear that, while increasing the concentration of CB[7] during synthesis, bigger particles are being formed to get finally rods shape in the addition of the spherical one. The broadness and shift in the absorption peak is due to rod shape of the AuNPs.

The effective diameter of the Au nanoparticles/nanorods obtained from DLS measurement was between 200 nm and 300 nm with a polydispersity of 0.25 (see Fig. 6A). Hence, when compared with the SEM images, the higher estimated size distribution in DLS analysis could be referred to the aggregation of the particles in the solution. For charge stabilized particles, the zeta potential is a measure of the particle's stability. It is a key parameter that reflects the stability of suspension since it will make a repulsive force, keeping the gold

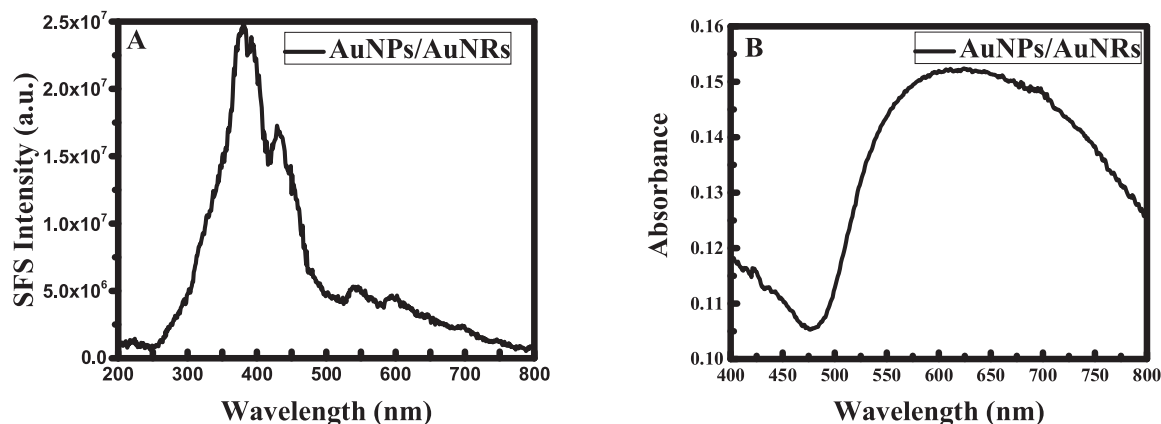


Fig. 2. Synchronous fluorescence spectra at $\Delta\lambda = 0$ nm (A) and UV–vis spectra (B) of curcumin functionalized Au nanoparticles/nanorods.

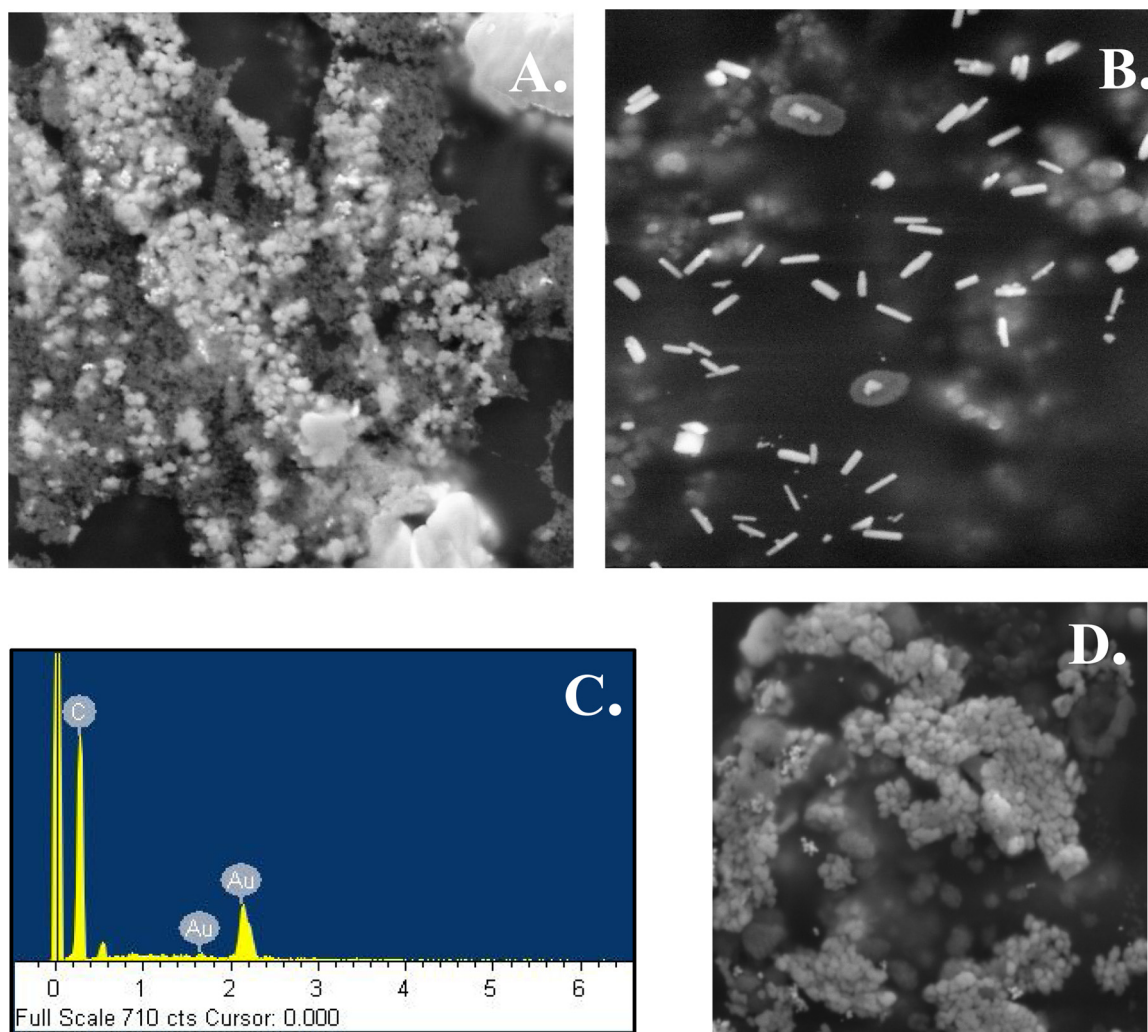


Fig. 3. SEM images of cucurbit [7] uril and curcumin functionalized gold nanoparticles (A), nanorods (B) and (C) corresponding EDX for the formed particles. (D) SEM image of cucurbit [6] uril and curcumin functionalized gold nanoparticles.

nanoparticles away from each other, which offers a high stability of suspension. In fact, nanoparticles with zeta potentials value > 20 mV or < -20 mV have sufficient electrostatic repulsion to remain stable in solution [27]. Fig. 6B shows the zeta potential measurement of the prepared gold nanoparticles. The result revealed that the value of the zeta potential of the AuNPs/AuNRs is -23.63 mV. This value is less than -20 mV verifying the formation of stable nanoparticles/nanorods without further precipitation within time.

The X-ray diffraction pattern was used to analyze the structure of

the Au nanoparticles/nanorods. The diffractograms of the prepared AuNPs/AuNRs, cucurbit[7]uril and curcumin is depicted in Fig. 7. XRD analysis showed four distinct diffraction peaks at 38.2° , 44.6° , 64.6° and 77.5° which indexed the plans 111, 200, 220 and 311 of the cubic face-centered gold. In fact, one sharp peak and another broad one at 14° and 23° respectively [28,29] belonging to CB[7] appear in the pattern indicating that AuNPs/AuNRs are stabilized and protected by CB[7] methylene group. As for the curcumin, the characteristics peaks appeared at diffraction angles of 2θ equal to 8.06° , 9.14° , 12.37° , 15.06°

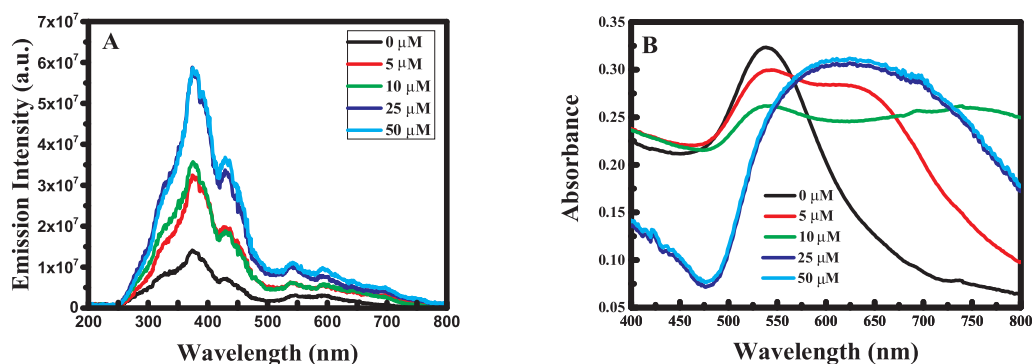


Fig. 4. Synchronous fluorescence spectra at $\Delta\lambda = 0$ nm (A) and UV-vis spectra (B) of cucurbit [7] uril and curcumin functionalized gold nanoparticles prepared at different concentrations of cucurbit [7] uril.

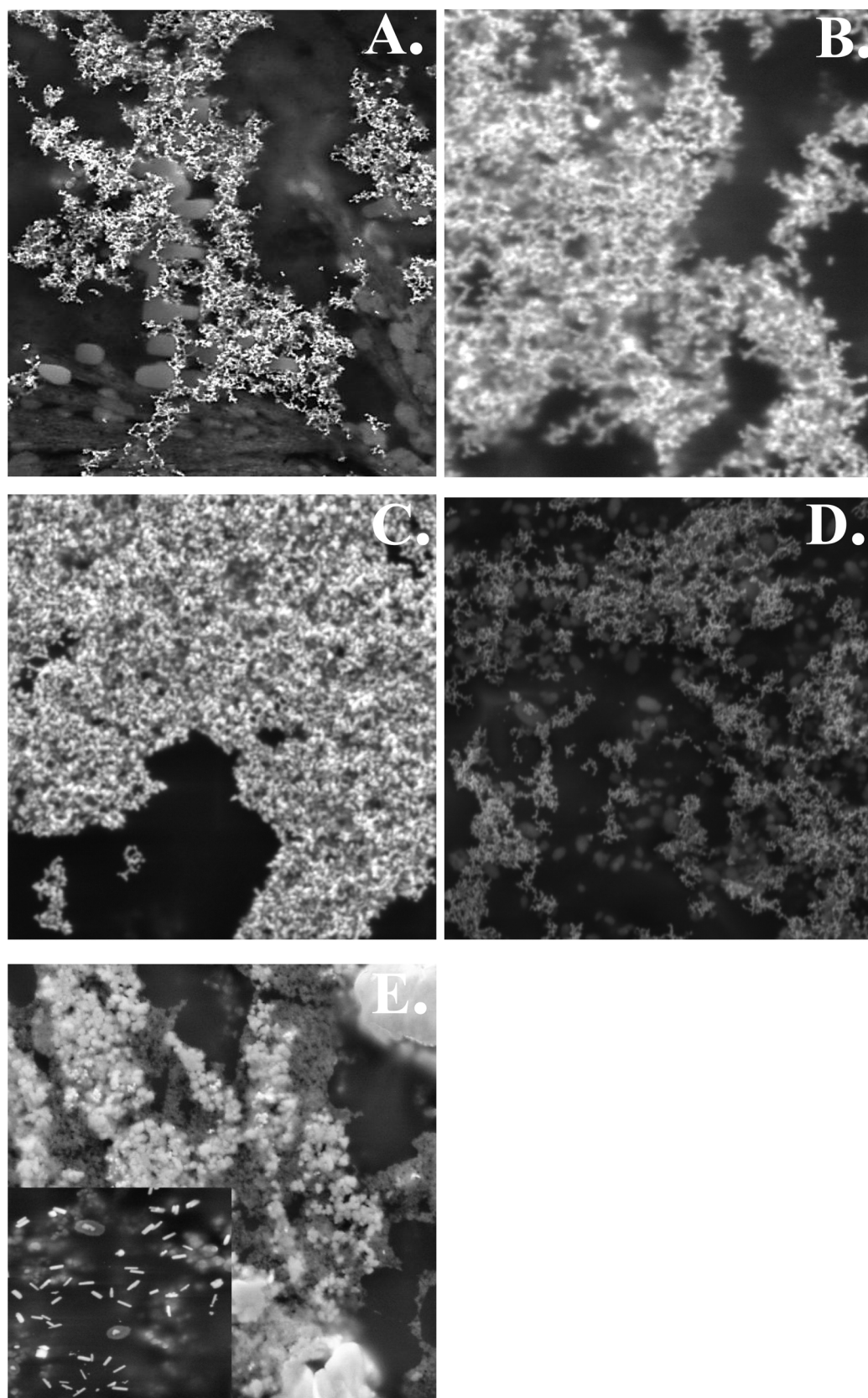


Fig. 5. SEM images of cucurbit [7] uril and curcumin functionalized gold nanoparticles prepared at different concentration of cucurbit[7]uril: (A) C = 1.0 μM ; (B) C = 5 μM ; (C) C = 10 μM ; (D) C = 25 μM and (E) C = 50 μM .

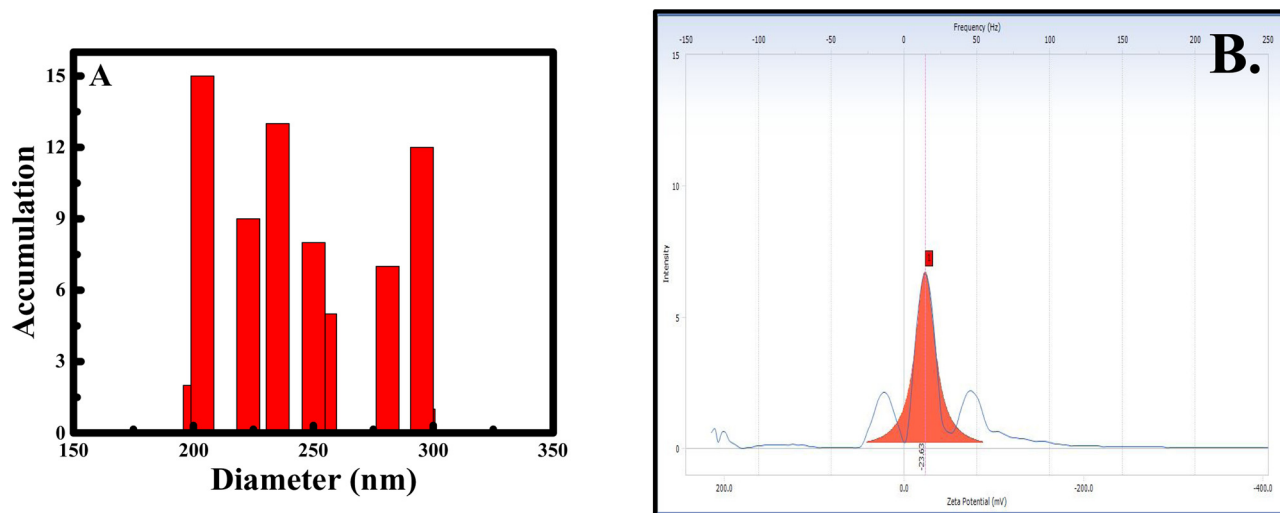


Fig. 6. Particle size distribution (A) and corresponding zeta potential value (B) of cucurbit [7] uril and curcumin functionalized gold nanoparticles.

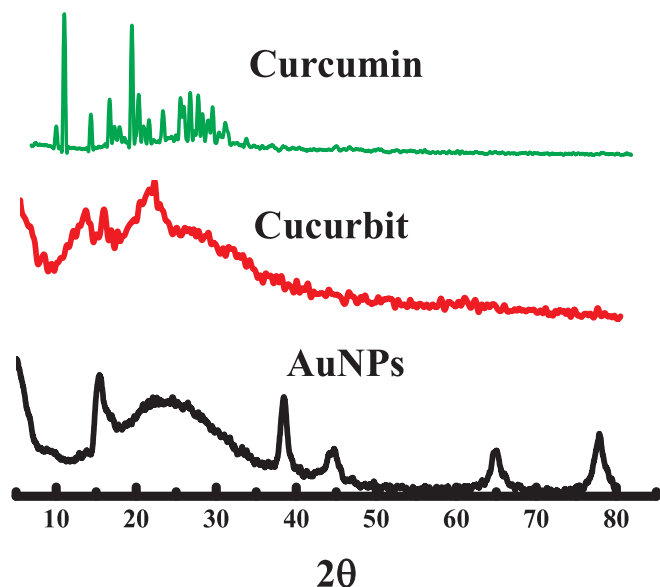


Fig. 7. X-ray diffraction pattern of cucurbit [7] uril and curcumin functionalized gold nanoparticles.

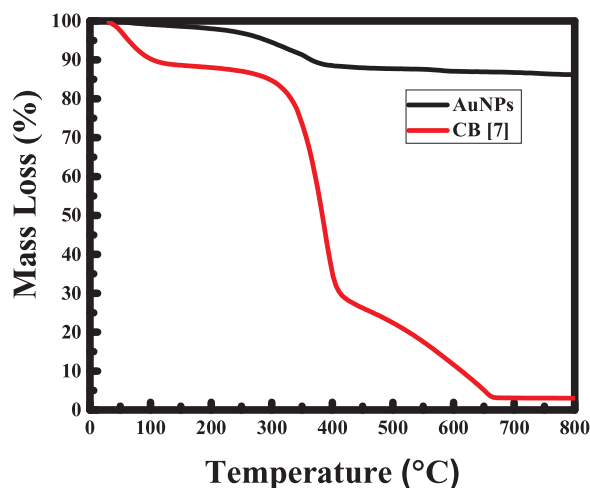


Fig. 8. TGA of cucurbit [7] uril and curcumin functionalized gold nanoparticles and cucurbit [7] uril.

and 17.75° indicating that curcumin is present in the crystalline form. Yet, it is found that the relative peaks of curcumin are absent in the spectrum of AuNPs/AuNRs, which suggests that curcumin peaks are too broadened and the XRD pattern is dominated by the structure of cucurbituril-AuNPs/AuNRs. To determine the binding amount of CB[7] present in the AuNPs, the prepared CB [7]-stabilized AuNPs/AuNRs were subjected to thermogravimetric analysis. It was found that the amount of CB[7] was approximately 25%. The TG curve of CB[7] depicted in Fig. 8 also shows a continuous decomposition with almost 100% mass loss around 600°C . This could induce the formation of inorganic core organic hybrid structures [18]. Interestingly, no loss of water was observed around 100°C , which assumes that the samples were dehydrated; thus, the AuNPs/AuNRs that were formed are stable.

The kinetics growth of the AuNPs/AuNRs was determined in two different ways, either by measuring the absorbance of AuNPs/AuNRs formed through following the synthesis by stopping the reaction in a given time interval and separating the AuNPs/AuNRs after centrifugation, or by monitoring the absorbance of curcumin in the reaction mixture before centrifugation. During the growth interval of AuNPs/AuNRs, the LSPR peak in the UV-vis spectrum was found to be $\sim 610\text{ nm}$ (See Fig. 9A) at $t = 10\text{ min}$ and it remained constant till end of the reaction. However, the absorbance at $\sim 610\text{ nm}$ increased till $t = 40\text{ min}$ and then remained constant till $t = 120\text{ min}$. The change in absorbance of AuNRs with time during synthesis is plotted in Fig. 9B. The estimated rate constant for the formation of AuNRs in this case was estimated as 0.019 min^{-1} , which gave a half-life value of 36 min. For the depletion of the curcumin concentration, the change of the absorbance during time was monitored at 425 nm . The absorbance of curcumin decreased remarkably with the formation of AuNRs and saturated after 10 min (See Fig. 9C). The rate of reduction in curcumin absorbance during the synthesis is depicted in Fig. 9D, where it is found that the rate constant for the depletion of curcumin concentration equal to 0.0693 min^{-1} with a half-life value of 10 min. The difference in the rate constant of AuNRs and the rate of depletion of curcumin could be due attributed to the degradation of curcumin during the reaction in alkaline media [30].

4. Conclusion

Curcumin has many pharmaceutical benefits. Earlier we have established curcumin as an attractive and alternative green reagent for the reduction of gold/silver salts to elemental gold/silver. Here it was shown that when curcumin was applied along with CB[7] as reducing and stabilizing agent, AuNRs are formed. Interestingly, AuNPs prepared

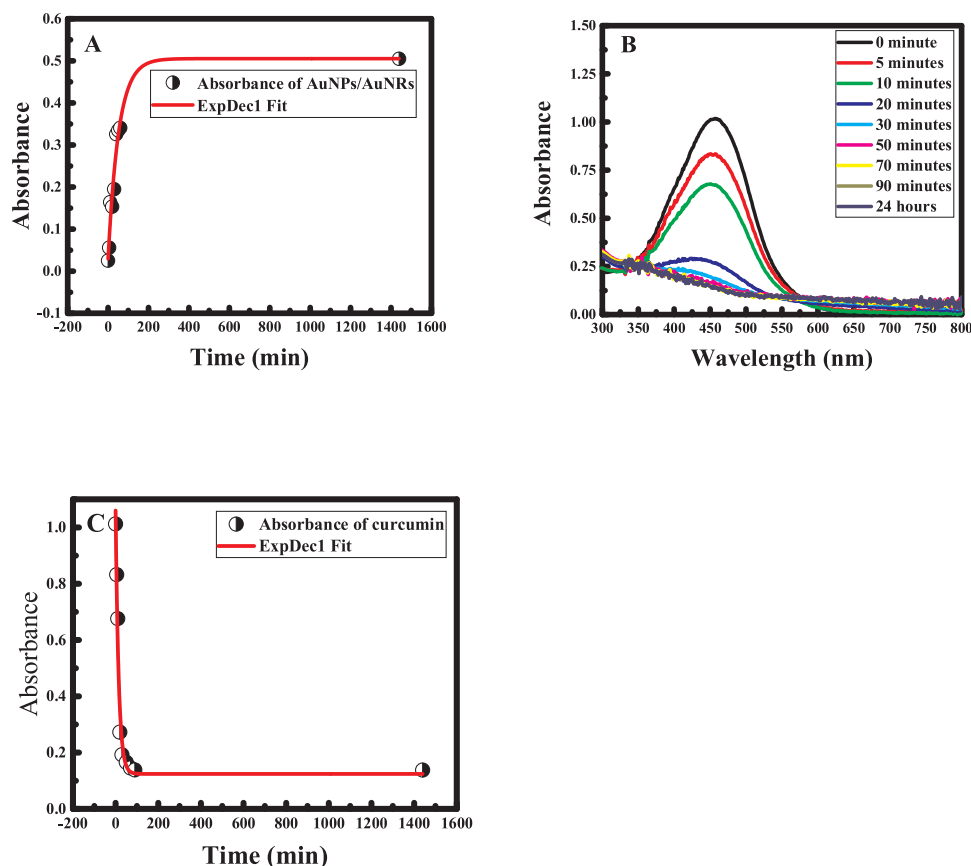


Fig. 9. Change in absorbance of AuNRs during its synthesis in extreme alkaline condition with time (A); absorption spectra of curcumin during synthesis of AuNRs (B); and change in absorbance of curcumin during synthesis of AuNRs with time (C).

using curcumin alone in aqueous environment offered spherical and smaller size, 10–20 nm, particles. On the other hand, when the same synthesis was carried out in the presence of CB[7], larger size NPs and at higher concentration of CB[7] Au NRs were formed. This was clearly evident from surface Plasmon resonance spectra in which AuNPs prepared without CB[7] gave a sharp spectrum peaked at ~536 nm and with CB[7] showed a broad spectrum peaked at ~610 nm. It was noted that higher concentration (~50 μM) of CB[7] is required to form AuNRs. Formation of AuNPs and AuNRs were established by XRD and conjugation of CB[7] and curcumin was confirmed by FT-IR and TGA data. DLS suggested these particles aggregate in solution to form particles between 200 nm and 300 nm with a polydispersity of 0.25. However, Zeta potential measurement confirmed that formation of stable nanoparticles/nanorods without further precipitation within time. Kinetic study proved that the half-life for the formation of AuNP/NRs was 3.6 times higher than that of degradation of curcumin during synthesis, which concludes that some amount of curcumin degrades on its own during this process besides acting as reducing agent.

Acknowledgments

Financial support provided by Lebanese National Council of Scientific Research (NCSR), Lebanon and American University of Beirut, Lebanon through URB as well as Kamal A. Shair Central Research Laboratory (KAS CRSL) facilities to carry out this work is greatly acknowledged.

References

- [1] Y. Sun, Y. Xia, Shape-controlled synthesis of Gold and silver nanoparticles, *Sci. Mag.* 298 (5601) (2002) 2176–2179, <http://dx.doi.org/10.1126/science.1077229>.
- [2] Y. Sun, Y. Xia, Alloying and dealloying processes involved in the preparation of metal nanoshells through a galvanic replacement reaction, *Nano Lett.* 3 (11) (2003) 1569–1572, <http://dx.doi.org/10.1021/nl034765r>.
- [3] H. Wang, D.W. Brandl, F. Le, P. Nordlander, N.J. Halas, Nanorice: a hybrid plasmonic nanostructure, *Nano Lett.* 6 (4) (2006) 827–832, <http://dx.doi.org/10.1021/nl060209w>.
- [4] Y.-C. Yeh, B. Creran, V.M. Rotello, Gold nanoparticles: preparation, properties, and applications in bionanotechnology, *Nanoscale* 4 (6) (2012) 1871–1880, <http://dx.doi.org/10.1039/C1NR11188D>.
- [5] M. Brust, M. Walker, D. Bethell, D.J. Schiffrin, R. Whyman, Synthesis of thiol-derivatised Gold nanoparticles in, *J. Chem. Soc. Chem. Commun.* (1994) 801–802, <http://dx.doi.org/10.1039/C39940000801>.
- [6] R. El Kurdi, D. Patra, The role of OH⁻ in the formation of highly selective gold nanowires at extreme pH: multi-fold enhancement in the rate of the catalytic reduction reaction by gold nanowires, *Phys. Chem. Chem. Phys.* 19 (7) (2017) 5077–5090, <http://dx.doi.org/10.1039/C6CP08607A>.
- [7] J. Pérez-Juste, I. Pastoriza-Santos, L.M. Liz-Marzán, P. Mulvaney, Gold nanorods: synthesis, characterization and applications, *Coord. Chem. Rev.* 249 (2005) 1870–1901, <http://dx.doi.org/10.1016/j.ccr.2005.01.030>.
- [8] B.E. Brinson, J.B. Lassiter, C.S. Levin, R. Bardhan, N. Mirin, N.J. Halas, Nanoshells made easy: improving Au layer growth on nanoparticle surfaces, *Langmuir* 24 (2008) 14166–14171, <http://dx.doi.org/10.1021/la802049p>.
- [9] J. Chen, F. Saeki, B.J. Wiley, et al., Gold nanocages: bioconjugation and their potential use as optical imaging contrast agents, *Nano Lett.* 5 (3) (2005) 473–477, <http://dx.doi.org/10.1021/nl047950t>.
- [10] N.L. Rosi, C.A. Mirkin, Nanostructures in biodiagnostics, *Chem. Rev.* 105 (4) (2005) 1547–1562, <http://dx.doi.org/10.1021/cr030067f>.
- [11] J. Lagona, P. Mukhopadhyay, S. Chakrabarti, L. Isaacs, The inverted cucurbit[n]uril family, *Angew. Chem. – Int. Ed.* 127 (51) (2005) 18000–18001, <http://dx.doi.org/10.1021/ja056988k>.
- [12] J. Kim, I.S. Jung, S.Y. Kim, et al., New cucurbituril homologues: syntheses, isolation, characterization, and X-ray crystal structures of cucurbit[n]uril (n = 5, 7, and 8), *J. Am. Chem. Soc.* 122 (3) (2000) 540–541, <http://dx.doi.org/10.1021/ja993376p>.
- [13] A. Day, A.P. Arnold, R.J. Blanch, B. Snushall, Controlling factors in the synthesis of cucurbituril and its homologues, *J. Org. Chem.* 66 (24) (2001) 8094–8100, <http://dx.doi.org/10.1021/jo015897c>.
- [14] E. Masson, X. Ling, R. Joseph, L. Kyeremeh-Mensah, X. Lu, Cucurbituril chemistry: a tale of supramolecular Success, *RSC Adv.* (2012), <http://dx.doi.org/10.1039/C1RA00768H>.
- [15] W.M. Nau, O.A. Scherman, The world of cucurbiturils – from peculiarity to commodity, *Isr. J. Chem.* 51 (5-6) (2011) 492–494, <http://dx.doi.org/10.1002/ijch>.

- 201100052.
- [16] S. Gürbüz, M. Idris, D. Tuncel, Cucurbituril-based supramolecular engineered nanostructured materials, *Org. Biomol. Chem.* 13 (2) (2015) 330–347, <http://dx.doi.org/10.1039/C4OB02065K>.
- [17] A. Corma, H. García, P. Montes-Navajas, A. Primo, J.J. Calvino, S. Trasobares, Gold nanoparticles in organic capsules: a supramolecular assembly of gold nanoparticles and cucurbituril, *Chem. – A Eur. J.* 13 (22) (2007) 6359–6364, <http://dx.doi.org/10.1002/chem.200601900>.
- [18] T. Premkumar, K.E. Geckeler, Cucurbit[7]uril as a tool in the green synthesis of gold nanoparticles, *Chem. – Asian J.* 5 (12) (2010) 2468–2476, <http://dx.doi.org/10.1002/asia.201000338>.
- [19] T.-C. Lee, O.A. Scherman, Formation of dynamic aggregates in water by cucurbit[5]uril capped with gold nanoparticles, *Chem. Commun.* 46 (14) (2010) 2438–2440, <http://dx.doi.org/10.1039/b925051d>.
- [20] D.K. Singh, R. Jagannathan, P. Khandelwal, P.M. Abraham, P. Poddar, In situ synthesis and surface functionalization of gold nanoparticles with curcumin and their antioxidant properties: an experimental and density functional theory investigation, *Nanoscale* 5 (5) (2013) 1882, <http://dx.doi.org/10.1039/c2nr33776b>.
- [21] R. El Kurdi, D. Patra, Amplification of resonance Rayleigh scattering of gold nanoparticles by tweaking into nanowires: bio-sensing of α -tocopherol by enhanced resonance Rayleigh scattering of curcumin capped gold nanowires through non-covalent interaction, *Talanta* 168 (January) (2017) 82–90, <http://dx.doi.org/10.1016/j.talanta.2017.03.021>.
- [22] S.S. Shankar, A. Rai, B. Ankamwar, A. Singh, A. Ahmad, M. Sastry, Biological synthesis of triangular gold nanoprisms, *Nat. Mater.* 3 (7) (2004) 482–488, <http://dx.doi.org/10.1038/nmat1152>.
- [23] S.P. Chandran, M. Chaudhary, R. Pasricha, A. Ahmad, M. Sastry, Synthesis of gold nanotriangles and silver nanoparticles using Aloe vera plant extract, *Biotechnol. Prog.* 22 (2) (2006) 577–583, <http://dx.doi.org/10.1021/bp0501423>.
- [24] B. Ankamwar, M. Chaudhary, M. Sastry, Gold nanotriangles biologically synthesized using tamarind leaf extract and potential application in vapor sensing, *Synth. React. Inorg. Met. Nano-Metal Chem.* 35 (1) (2005) 19–26, <http://dx.doi.org/10.1081/SIM-200047527>.
- [25] E. Shaabani, S.M. Amini, S. Kharrazi, R. Tajerian, Curcumin coated gold nanoparticles: synthesis, characterization, cytotoxicity, antioxidant activity its comparison with citrate coat Gold, *Nanoparticles* 4 (2) (2017) 115–125, <http://dx.doi.org/10.22038/nmj.2017.21506.1227>.
- [26] F. Abdulwahab, F.Z. Henari, S. Cassidy, K. Winsor, Synthesis of Au, Ag, curcumin Au/Ag, and Au-Ag nanoparticles and their nonlinear refractive index properties, *J. Nanomater.* (2016) 1–8, <http://dx.doi.org/10.1155/2016/5356404>.
- [27] L.H. Bac, J.S. Kim, J.C. Kim, Size, optical and stability properties of gold nanoparticles synthesized by electrical explosion of wire in different aqueous media, *Rev. Adv. Mater. Sci.* 28 (2) (2011) 117–121.
- [28] F. Constabel, K.E. Geckeler, Solvent-free self-assembly of C60 and cucurbit[7]uril using high-speed vibration milling, *Tetrahedron Lett.* 45 (10) (2004) 2071–2073, <http://dx.doi.org/10.1016/j.tetlet.2004.01.071>.
- [29] G.C. Bolfarini, M.P. Siqueira-Moura, G.J.F. Demets, A.C. Tedesco, Preparation, characterization, and in vitro phototoxic effect of zinc phthalocyanine cucurbit[7]uril complex encapsulated into liposomes, *Dye Pigment* 100 (1) (2014) 162–167, <http://dx.doi.org/10.1016/j.dyepig.2013.08.018>.
- [30] E.D. El Khoury, D. Patra, Ionic liquid expedites partition of curcumin into solid gel phase but discourages partition into liquid crystalline phase of 1,2-dimyristoyl-sn-glycero-3-phosphocholine liposomes, *J. Phys. Chem. B* 117 (33) (2013) 9699–9708, <http://dx.doi.org/10.1021/jp4061413>.